Hydrodynamics of lattice-gas automata

Gianluigi Zanetti
The James Franck Institute, The University of Chicago, 5640 South Ellis Avenue, Chicago, Illinois 60637
(Received 4 October 1988)

The linear and nonlinear hydrodynamics of the two-dimensional lattice-gas automata (LGA) are discussed. The physics of the LGA is found to be richer than previously expected. Together with sound and shear waves (characteristic of simple fluids) there are three new hydrodynamic modes. The conserved quantities corresponding to the latter arise from a feature of the microscopic definition of the LGA; i.e., the particles of the microscopic gas occupy the sites of a regular lattice and can only hop from one site to its nearest neighbors. The presence of these new conserved quantities has unexpected results on the macroscopic behavior of the fluid. In fact, there is a nonlinear coupling between the two classes of modes, and while the new conserved densities are merely convected by the momentum density, the current of the latter contains terms that depend only on the new modes. Thus the presence of a finite amount of the new conserved densities produces flow patterns that are not solutions of the Navier-Stokes equation. Although only the two-dimensional hexagonal-lattice gas is discussed, the arguments described here apply with equal force to currently proposed three-dimensional models.

I. INTRODUCTION

Lattice-gas automata[1] (LGA) have been recently proposed as an alternate technique for the numerical solution of the Navier-Stokes equation. They are discrete microscopic models which can be easily simulated on a computer and whose macroscopic behavior is similar to that of simple real fluids. The practical advantages of such a technique are many, e.g., intrinsic numerical stability,[2] extreme parallelism.[3] It has not been definitively clarified,[4] however, whether the hydrodynamic behavior of the LGA can be really mapped into solution of the Navier-Stokes equation, and if this new technique is actually more "economical" than the standard approaches for the numerical solution of partial differential equation,[5] e.g., finite-difference schemes.[6]

In its simplest form the lattice-gas automaton is a gas of particles that occupy the sites of a regular lattice and can hop from the lattice sites to their nearest neighbors. The particles can collide only on the lattice sites and the possible collisions are described by a set of deterministic rules. In a collision, the particles are scattered between the possible hopping directions, leaving the number and linear momentum of the particles present at each site intact. The transition from the microscopic to the macroscopic description of the LGA is done by defining coarse-grained conserved densities, e.g., momentum density, obtained by averaging their microscopic equivalents over subregions of the lattice. The presence of microscopic conservation laws then reappears in the macroscopic dynamic as hydrodynamic modes and, when the underlying regular lattice has been properly chosen, it is usually argued that the form of the hydrodynamic equations is very similar to that found for simple fluids.

The hydrodynamic description of the LGA has been the subject of numerous papers.[1,2,7] Unfortunately, until Ref. 8, the list of conserved densities has been incomplete. In fact, the macroscopic behavior of the LGA models currently proposed is richer than expected. Together with the conservation laws imposed by the choice of collision rules, there are other extensive invariants which are a pecularity of the discretized dynamics of the LGA. The presence of these new invariants can be easily understood by using a trivial one-dimensional example. Let $g(x)$ be the linear momentum of the particles present at site x, define $G_e(t)=\sum_{x\ \mathrm{even}} g(x,t)$, $G_o(t)=\sum_{x\ \mathrm{odd}} g(x,t)$ as the total momentum of the particles on even or odd sites, and let the collision rules conserve the momentum and the number of particles at each site. Since the particles can only hop between nearest neighbors, G_e and G_o are exchanged at each time step. The dynamics of this one-dimensional model allows three conserved quantities: M, G_e+G_o, and $H=(-1)^t(G_e-G_o)$. The first two are the usual total number of particles and the total linear momentum; the third is due to our extremely simplified dynamics.

The conserved quantity H can be easily generalized to the two- and three-dimensional LGA. However, we will restrict ourselves to the discussion of the two-dimensional model described in Ref. 9. The analog of H in this model is three conserved quantities H_a, where $a=1,2,3$, with corresponding microscopic densities h_a. In this paper, I discuss the implications of these new conserved quantities for the macroscopic behavior of the LGA fluid. The main result of this work is Eq. (24), the constitutive equation for the two-dimensional lattice gas. The most striking feature of Eq. (24) is the presence of a nonlinear coupling between the two classes of hydrodynamic modes.[10] Although the h densities are merely convected, albeit in an anisotropic fashion, by the momentum density g_m, the expression for the time derivative of g_m, Eq. (22), contains a term that depends only on h. Thus the presence

of a finite amount of the h density produces flow patterns which are not solutions of the Navier-Stokes equation. On the other hand, since the current for the h_a, Eq. (23), is zero for $h_a=0$, the presence of the h_a depends on the initial conditions used for the LGA simulation. Although only the two-dimensional hexagonal-lattice gas is discussed; the arguments described here and the relevant results apply with equal force to the currently proposed three-dimensional models.

The paper is organized as follows. In Sec. II I discuss the linearized hydrodynamics of the LGA. The formalism used is from Ref. 12 and the detailed concerning the relevant calculations are relegated to Appendix A. In Sec. II I give the linearized version of Eq. (22), which is best[8] expressed by the linearized hydrodynamic matrix,[13] Eq. (10'). Equation (10') indicates that the new conserved densities h_a, $a=1,2,3$ have a nonisotropic diffusive behavior. This is not surprising since the h are strongly related to the underlying lattice. Equation (10') shows also that there is no linear coupling between the "standard" hydrodynamics modes of the LGA, i.e., sound and shear waves and the h_a. At the end of Sec. II I give a Green-Kubo expression for κ_1 and κ_2, and h modes transport coefficients, together with their Chapman-Enskog values. In Fig. 1, I compare the transport coefficients obtained by direct simulations with their Chapman-Enskog analogs. Both the Green-Kubo expression Eq. (16) and the Chapman-Enskog formula Eq. (17) are new. Section III extends the previous one to include the nonlinear coupling between conserved densities of the model. Here the main result is Eq. (24), the "Eulerian" contribution to the LGA hydrodynamic constitutive relations. Equation (24) is obtained by keeping the first two orders of a perturbative expansion in the intensive parameters conjugated to the momentum density and the h_a-mode density. Once again the details are relegated to Appendix B. The effects of the unexpected nonlinear coupling between the two classes of modes are illustrated by a simulation, whose results are depicted in Fig. 2. Section IV contains conclusions.

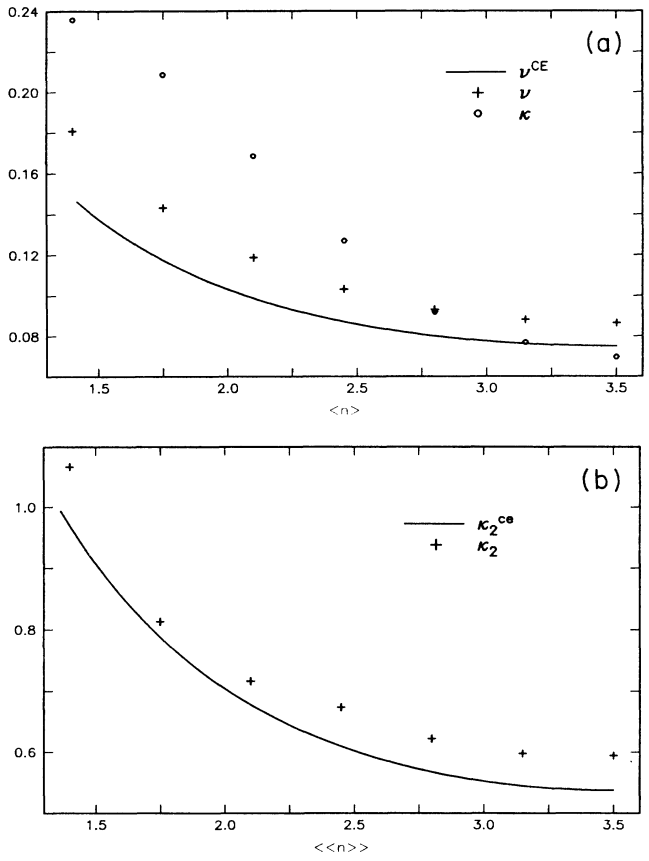

FIG. 1. (a) Plot of κ_1, obtained from a forced-flow measurement, as a function of the average number of particles per lattice site. The set of collision rules used in the simulations is the FHP-III described in Ref. 9. The solid line is the Chapman-Enskog estimate for κ_1^{CE} given in the text. Together with κ_1 (+), I plotted the kinematic viscosity ν^{CE} (○), cf. the end of Sec. II. The data for ν are from Ref. 19. (b) Plot of κ_2, obtained from a forced-flow measurement, as a function of the average number of particles per lattice site. The set of collision rules used in the simulations is the FHP-III described in Ref. 9. The solid line is the Chapman-Enskog estimate for κ_2^{CE} given in the text.

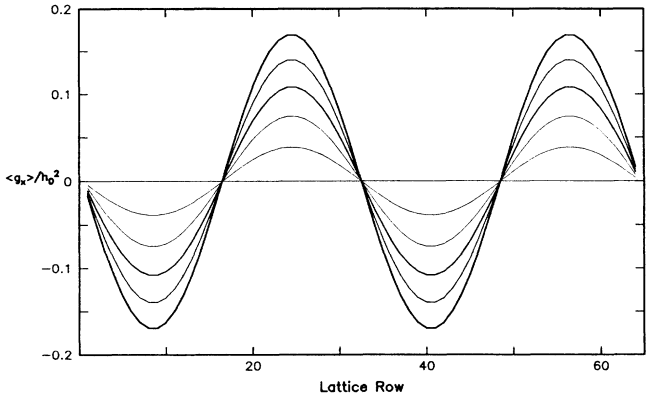

FIG. 2. Simulation with "pathological" initial conditions, $\langle h_2 \rangle = h_0 \sin(2\pi y/W)$ and $\langle g_m \rangle = 0$, in a two-dimensional box with periodic boundary conditions. The coordinate axes are oriented so that $\hat{\mathbf{x}} \| \mathbf{C}_1$ and the box is a parallelogram of width (y direction) W and length L. The solid curves plotted are the momentum density $\langle g_x \rangle / h_0^2$ vs y. The time difference between curves is five microscopic time steps. The actual size of the system used is $L=2$, $W=64$, the set of collision rules used in the simulations is the FHP-III described in Ref. 9, and the simulation is performed using a recently developed Boltzmann-equation technique (Ref. 24).

II. LINEARIZED HYDRODYNAMICS OF THE LGA

A. Microscopic description of the model

The two-dimensional lattice-gas automation is defined as a gas of particles that occupy the sites of a regular hexagonal lattice and that can hop from a site to its nearest neighbors. The hopping is formally described by assign-

ing to each particle a velocity selected from the seven-velocity vectors $\mathbf{C}_a=(\cos[\pi(a-1)/3],\sin[\pi(a-1)/3])$, $a=1,\ldots,6$ and $\mathbf{C}_0=(0,0)$. (Here and in the following we take the abscissa axis to be oriented parallel to $\mathbf{C}_1$.) To simplify the model even further, no more than one particle is allowed to have a given velocity at a given site. Thus the microscopic population density $f_a(\mathbf{r},t)$ is a Boolean variable that indicates the presence (1) or the absence (0) of a particle of velocity $\mathbf{C}_a$ at site $\mathbf{r}$ and time step t.

The time evolution of the system is described as the composition of a collision operator with a streaming operator. The streaming operator describes the hopping of the particles in the direction of their velocities, while the collision operator conserves the total number of particles and the total momentum at any given site. Thus

$$\begin{aligned}&\sum_a f_a(\mathbf{r},t+1)=\sum_a f_a(\mathbf{r}-\mathbf{C}_a,t)\ ,\\&\sum_a C_{a;m}f_a(\mathbf{r},t+1)=\sum_a C_{a;m}f_a(\mathbf{r}-\mathbf{C}_a,t)\ .\end{aligned}\tag{1}$$

I will use the convention that $a,b,c,\ldots$, label the microscopic velocities, while $i,j,k,\ldots$, label the Cartesian coordinates. Repeated indices imply summation. I will also define $\mathcal{L}$ as the time evolution operator obtained by the composition of the collision and streaming ones.[14,15] The order in which the collision and the streaming operator are composed is arbitrary; however, it does not affect the results.

The total number of particles of the system $M=\sum_{\mathbf{r}\in\Omega}\sum_a f_a(\mathbf{r})$ and the total linear momentum $G_m=\sum_{\mathbf{r}\in\Omega}\sum_a C_{a;m}f_a(\mathbf{r})$ are clearly conserved. Ω indicates both the region of the hexagonal lattice occupied by the system and its volume. A less trivial invariant is the total staggered momentum

$$H_a=(-1)^t\sum_{\mathbf{r}\in\Omega}(-1)^{\mathbf{B}_a\cdot\mathbf{r}}\mathbf{C}_a^{\perp}\cdot\mathbf{g}(\mathbf{r},t)\ ,\tag{2}$$

where $\mathbf{C}_a^{\perp}$ is obtained by rotating $\mathbf{C}_a$ by $\pi/4$ counterclockwise, $\mathbf{B}_a$ is the reciprocal space vector perpendicular to $\mathbf{C}_a$, i.e., $\mathbf{B}_a=(2/\sqrt{3})\mathbf{C}_a^{\perp}$. I also have introduced the microscopic momentum density $g_m(\mathbf{r},t)=\sum_a C_{a;m}f_a(\mathbf{r},t)$. Later we will need the density of mass $n(\mathbf{r},t)=\sum_a f_a(\mathbf{r},t)$ and the staggered-momentum density

$$h_a(\mathbf{r},t)=(-1)^t(-1)^{\mathbf{B}_a\cdot\mathbf{r}}\mathbf{C}_a^{\perp}\cdot\mathbf{g}(\mathbf{r},t)\ .$$

The index a in H_a runs over $1,\ldots,6$, but $H_{a+3}=-H_a$ and thus it is enough if we choose $a=1,2,3$. Equation (2) can be verified by inspection[16] and gives, together with N and G_m, six extensive invariants.

In the following, the physically relevant formulas are expressed in terms of thermodynamic equilibrium averages. The latter, indicated by $\langle\langle\ \rangle\rangle$, should be understood as averages on the grand canonical ensemble

$$\langle\langle f\rangle\rangle_{\alpha,\gamma,\eta}=\sum_x p_x(\alpha,\gamma,\eta)f_x\ ,\tag{3}$$

where x indicates a possible microscopic configuration of the LGA, f_x is the quantity f, e.g., $g_m(\mathbf{r})$, calculated on x. The weight $p_x(\alpha,\gamma,\eta)$ is the grand canonical weight

$$\begin{aligned}&p(\alpha,\gamma,\eta)=\frac{e^{\alpha M-\gamma\cdot\mathbf{G}-\eta_a H_a}}{Z(\alpha,\gamma,\eta)}\ ,\\&Z(\alpha,\gamma,\eta)=\sum_x e^{\alpha M-\gamma\cdot\mathbf{G}-\eta_a H_a}\ .\end{aligned}\tag{4}$$

The intensive parameters α,γ,η completely determine the average values of the conserved densities. However, due to the discrete nature of the model (i.e., its lack of Galilean invariance), the behavior of fluctuations around the equilibrium is not independent of the equilibrium average value of g_m and h_a. This does not constitute a problem since[2] I will only compute averages on the equilibrium state described by γ, $\eta=0$, and $\alpha=\alpha_0$, where the average number of particles per site is $\langle\langle n(\mathbf{r})\rangle\rangle_{\alpha_0,0,0}=n_0=7d$, and write $\langle\langle f\rangle\rangle=\langle\langle f\rangle\rangle_{\alpha_0,0,0}$. Note that for these values of the intensive parameters, Eq. (4) completely factorizes on the sites and directions and has the hexagonal symmetry of the underlying lattice (see Appendix A).

B. Linearized hydrodynamics

Here, as in Appendixes A and B, I use the formalism of Ref. 12. A microscopic state of the LGA is indicated with $|x\rangle$ and the state of the system is expressed as a formal sum on all the microscopic states of the system, each weighted by their probability, e.g., the state of the system at time step t is $|t\rangle=\sum_x p_x(t)|x\rangle$. The application of $\mathcal{L}$ on $|t\rangle$ is defined as $\mathcal{L}|t\rangle=\sum_x p_{\mathcal{L}^{-1}x}(t)|x\rangle$ (see Appendix A). The Liouville equation is then $|t+1\rangle=\mathcal{L}|t\rangle$, i.e., $p_x(t+1)=p_{\mathcal{L}^{-1}x}(t)$.

To obtain the linearized hydrodynamic of the LGA we have to find its hydrodynamic modes, i.e., long wavelength, slowly relaxing, eigenvectors

$$|\Psi(\mathbf{q}),t\rangle=e^{-s(q)t}|\Psi(\mathbf{q})\rangle$$

of the Liouville operator $\mathcal{L}$,

$$e^{-s(\mathbf{q})}|\Psi(\mathbf{q})\rangle=\mathcal{L}|\Psi(\mathbf{q})\rangle\ .\tag{5}$$

The eigenvector $|\Psi(\mathbf{q}),t\rangle$ can be split, Appendix A, into two "orthogonal" parts. The first is obtained by projecting $|\Psi(\mathbf{q}),t\rangle$ on the analogous Fourier components of the conserved density fluctuations

$$\begin{aligned}&n(\mathbf{q})=\frac{1}{\sqrt{N}}\sum_{\mathbf{r}\in\Omega}e^{-i\mathbf{q}\cdot\mathbf{r}}[n(\mathbf{r})-n_0]\ ,\\&g_m(\mathbf{q})=\frac{1}{\sqrt{N}}\sum_{\mathbf{r}\in\Omega}e^{-i\mathbf{q}\cdot\mathbf{r}}g_m(\mathbf{r})\ ,\\&h_a(\mathbf{q})=\frac{1}{\sqrt{N}}\sum_{\mathbf{r}\in\Omega}e^{-i\mathbf{q}\cdot\mathbf{r}}h_a(\mathbf{r})\ ,\end{aligned}\tag{6}$$

where N is the total number of sites in the system. This projection can be written in a more compact way by defining the operator

$$P(\mathbf{q})=\sum_{\phi}\frac{|\phi(\mathbf{q})\rangle\langle\phi(\mathbf{q})|}{\langle\phi(\mathbf{q})|\phi(\mathbf{q})\rangle}\ ,\tag{7}$$

where ϕ runs over $\{n,g_m,h_a\}$, $\langle\Phi|\Psi\rangle=\langle\langle\bar{\Phi}\Psi\rangle\rangle$, $\langle\langle\Phi\rangle\rangle$ is the equilibrium average of the quantity Φ, and $\bar{\Phi}$ is the complex conjugate of Φ. For future reference we also define the susceptibilities $\chi_\phi=\langle\phi(\mathbf{q})|\phi(\mathbf{q})\rangle$ and the complement of $P(\mathbf{q})$,

$$Q(\mathbf{P})=1-P(\mathbf{q})\ .\tag{8}$$

The conserved density fluctuations of Eq. (6) are not eigenvectors of $\mathcal{L}$ for any finite q, but they are good approximations, to $O(q)$, of eigenvectors of $\mathcal{L}$. By adding to them an appropriate correction of $O(q)$ we can construct a better approximation, correct to $O(q^2)$, to an eigenvector of $\mathcal{L}$ and thus obtain an estimate for the eigenvalue which is correct up to $O(q^4)$. This suggests that it is possible to recast the eigenvalue equation, Eq. (5), into a more manageable form where only the local equilibrium-conserved quantities enter. In fact, Eq. (5) can be transformed (Appendix A) into

$$e^{-s(\mathbf{q})}P(\mathbf{q})|\Psi(\mathbf{q})\rangle = P(\mathbf{q})\mathcal{L}P(\mathbf{q})|\Psi(\mathbf{q})\rangle + P(\mathbf{q})\mathcal{L}Q(\mathbf{q})\frac{1}{e^{-s(\mathbf{q})}-Q(\mathbf{q})\mathcal{L}Q(\mathbf{q})} \times Q(\mathbf{q})\mathcal{L}|\Psi(\mathbf{q})\rangle \ , \tag{9}$$

and finally, by projecting Eq. (9) on the $|\phi(\mathbf{q})\rangle$ modes, I can express the decay rates $s(\mathbf{q})$ as solutions of

$$\det[(e^{-s(\mathbf{q})}-1)\delta_{\phi\phi'}-L_{\phi\phi'}(\mathbf{q})-U_{\phi\phi'}(\mathbf{q})]=0 \ . \tag{10}$$

The matrices $L_{\phi\phi'}(\mathbf{q})$ and $U_{\phi\phi'}(\mathbf{q})$ are

$$L_{\phi\phi'}(\mathbf{q})=iq_m \lim_{q\to 0}\frac{\langle J_m^{\phi}(\mathbf{q})|\phi'(\mathbf{q})\rangle}{\sqrt{\chi_{\phi}\chi_{\phi'}}} \ , \tag{11}$$

$$U_{\phi\phi'}(\mathbf{q})=\frac{q_i q_j}{\sqrt{\chi_{\phi}\chi_{\phi'}}} \times\left[D_{ij}^{\phi\phi'}+\lim_{q\to 0}\sum_{t=0}^{\infty}\langle J_i^{\phi}|Q(\mathbf{q})\mathcal{L}^t Q(\mathbf{q})J_j^{\phi'}(\mathbf{q})\rangle\right] , \tag{12}$$

where $J_j^{\phi}(\mathbf{q})$ is the microscopic current of the density ϕ along the Cartesian vector $\hat{\mathbf{j}}$, and we neglect, in Eqs. (11) and (12), terms $O(q^3)$. The $D_{ij}^{\phi\phi'}$ are corrections to the transport coefficient due to the discreteness of the model and they are explicitly given in Appendix A.

In Eq. (10) we split the matrix to be diagonalized into two parts. The "Euler" term $L_{\phi\phi'}$ is a streaming contribution which is completely contained in the equilibrium statistical mechanics of the LGA. In the case at hand, only the $\phi=n,\phi'=g_m$ elements of $L_{\phi\phi'}$ are not null. They represent the coupling between the longitudinal fluctuations of momentum density and number density fluctuations, i.e., the presence of sound waves. In contrast to $L_{\phi\phi'}$, $U_{\phi\phi'}$ is directly related to equilibrium correlation functions between the microscopic currents conjugated to the density $\phi(\mathbf{q})$ and $\phi'(\mathbf{q})$ and therefore contains information on the dynamics of the system. Formulas (11) and (12) allow us to bridge the microscopic description of the lattice-gas automaton to its macroscopic hydrodynamics. By comparing Eq. (12) to its macroscopic equivalent,[13] we can obtain the Green-Kubo expressions for the kinematic velocity ν and the second viscosity ζ, i.e.,

$$\nu=\frac{1}{\chi_g}\sum_{\mathbf{r}\in\Omega}\sum_{t=0}^{\infty}\langle\tilde{J}_y^x(0,0)|\tilde{J}_y^x(\mathbf{r},t)\rangle+\nu_s \ , \tag{13a}$$

$$\nu+\zeta=\frac{1}{\chi_g}\sum_{\mathbf{r}\in\Omega}\sum_{t=0}^{\infty}\langle\tilde{J}_y^y(0,0)|\tilde{J}_y^y(\mathbf{r},t)\rangle+\nu_s+\zeta_s \ , \tag{13b}$$

where the transverse microscopic current $\tilde{J}_j^i$ is given by

$$\tilde{J}_j^i(\mathbf{r},t)=\sum_a (C_{a;i}C_{a;j}-c_s^2\delta_{ij})(f_a(\mathbf{r},t)-d) \ , \tag{14}$$

c_s is the speed of sound for the lattice gas, and ν_s and ζ_s are corrections to the transport coefficients due to the discrete nature of the model.[17,18] While expressions similar to Eqs. (13a) and (13b) were given in Ref. 17, we have a new result in the expression for the diffusion coefficient for the h_a modes. In fact, it is easy to show, using the hexagonal symmetry of the lattice (Appendix A), that

$$U_{ab}(\mathbf{q})=\delta_{ab}q^2\kappa(\hat{q})=\delta_{ab}q^2[\kappa_1+\kappa_2(\hat{\mathbf{q}}\cdot\mathbf{C}_a^{\perp})^2] \tag{15}$$

with

$$\kappa_1=\frac{1}{\chi_h}\sum_{\mathbf{r}\in\Omega}\sum_{t=0}^{\infty}(-1)^t(-1)^{\mathbf{B}_a\cdot\mathbf{r}} \times\langle\tilde{J}_y^x(0,0)|\tilde{J}_y^x(\mathbf{r},t)\rangle+\kappa_{1,s} \ , \tag{16a}$$

$$\kappa_1+\kappa_2=\frac{1}{\chi_h}\sum_{\mathbf{r}\in\Omega}\sum_{t=0}^{\infty}(-1)^t(-1)^{\mathbf{B}_a\cdot\mathbf{r}} \times\langle\tilde{J}_y^y(0,0)|\tilde{J}_y^y(\mathbf{r},t)\rangle+\kappa_{1,s}+\kappa_{2,s} \ , \tag{16b}$$

where the κ_s are corrections due to the discrete nature of the model, $\kappa_{1,s}=\nu_s=-\frac{1}{8}$ and $\kappa_{2,s}=-\frac{1}{4}$. Having identified the various pieces of Eq. (10) with their macroscopic equivalents we can summarize Eq. (10) in the more compact form given below:

$$L_{\phi\phi'}(q)= \begin{array}{c} \\ n \\ g_x \\ g_y \\ h_1 \\ h_2 \\ h_3 \end{array} \begin{array}{c} \begin{array}{cccccc} n & g_x & g_y & h_1 & h_2 & h_3 \end{array} \\ \begin{bmatrix} 0 & ic_sq_x & ic_sq_y & 0 & 0 & 0 \\ ic_sq_x & -(\zeta q_x^2+\nu q^2) & -\zeta q_xq_y & 0 & 0 & 0 \\ ic_sq_y & -\zeta q_xq_y & -(\zeta q_y^2+\nu q^2) & 0 & 0 & 0 \\ 0 & 0 & 0 & -q^2\kappa_1(\hat{\mathbf{q}}) & 0 & 0 \\ 0 & 0 & 0 & 0 & -q^2\kappa_2(\hat{\mathbf{q}}) & 0 \\ 0 & 0 & 0 & 0 & 0 & -q^2\kappa_3(\hat{\mathbf{q}}) \end{bmatrix} \end{array} \tag{10'}$$

The symbols c_s, ν, and ζ indicate, respectively, the speed of sound, the kinematic viscosity, and the second viscosity of the LGA fluid. The transport coefficients for the h_a densities are anisotropic, i.e., $\kappa_a(\hat{\mathbf{q}})=\kappa_1+\kappa_2(\hat{\mathbf{q}}\cdot\mathbf{C}_a^{\perp})^2$.

In contrast to ν and ζ, κ has a nontrivial angular dependence $\kappa=\kappa(\hat{\mathbf{q}})$. In fact, the h_a modes are a peculiarity of the microscopic definition of the model and thus it is not surprising that this is reflected in the symmetries of their transport coefficients. The diffusion coefficients κ_1 and κ_2 can be directly obtained by using a forced-flow technique similar to that used in Refs. 19 and 20. In Fig. 1 these coefficients are plotted as a function of the average number of particles per lattice site. The set of collision rules used in the simulations is FHP-III described in Ref. 9. The solid lines in Fig. 1 are the Chapman-Enskog estimate for $\kappa_1^{\mathrm{CE}},\kappa_2^{\mathrm{CE}}$,

$$\kappa_1^{\mathrm{CE}}=\frac{1}{28\hat{d}(1-7/8\hat{d})}+\kappa_{s,1}\ , \tag{17}$$

$$\kappa_1^{\mathrm{CE}}+\kappa_2^{\mathrm{CE}}=\frac{3(2-11\hat{d}+32\hat{d}^2-44\hat{d}^3+32\hat{d}^4)}{4\hat{d}(6-29\hat{d}+66\hat{d}^2-48\hat{d}^3)}+\kappa_{s,1}+\kappa_{s,2}\ , \tag{18}$$

with $\hat{d}=d(1-d)$. Equations (17) and (18) are obtained[21] using a technique similar to the one described in Ref. 18.

The formula given above for κ_1^{CE} is exactly the Chapman-Enskog estimate for the kinematic viscosity ν^{CE} Ref. 9. On the other hand, the Green-Kubo expression for ν, Eq. (13a), is clearly different from Eq. (16a). The coincidence between the Chapman-Enskog estimates of the transport coefficients κ_1 and ν is, however, not surprising. To support this statement we can use the following heuristic argument. Rivet[22] argues that, in the Boltzmann-equation approximation, the correlation function on the right-hand side of Eq. (13a) can be estimated as

$$\nu-\nu_s\approx\frac{\langle\tilde{J}_y^x(0)|\tilde{J}_y^x(0)\rangle}{\langle\tilde{J}_y^x(0)|\tilde{J}_y^x(0)\rangle-\langle\tilde{J}_y^x(0)|\mathcal{L}\tilde{J}_y^x(0)\rangle}=\nu^{\mathrm{CE}}-\nu_s\ , \tag{19}$$

where

$$\langle\tilde{J}_y^x(0)|\tilde{J}_y^x(t)\rangle=\frac{1}{N}\sum_{\mathbf{r},\mathbf{r}'}\langle\tilde{J}_y^x(\mathbf{r},0)\tilde{J}_y^x(\mathbf{r}',t)\rangle\ . \tag{20}$$

It is easy to show that

$$(-1)^1\sum_{\mathbf{r}\in\Omega}(-1)^{\mathbf{B}_a\cdot\mathbf{r}}\langle\tilde{J}_y^x(\mathbf{0},0)|\mathcal{L}\tilde{J}_y^x(\mathbf{r},0)\rangle=\sum_{\mathbf{r}\in\Omega}\langle\tilde{J}_y^x(\mathbf{0},0)|\mathcal{L}\tilde{J}_y^x(\mathbf{r},0)\rangle\ . \tag{21}$$

Thus, using the analog of Eq. (13a), i.e., Eq. (16a), to estimate κ_1^{CE}, we obtain $\kappa^{\mathrm{CE}}=\nu^{\mathrm{CE}}$. This rough argument gives one some intuition into why there is no difference between κ^{CE} and ν^{CE}. However, the full value of ν,κ_1 obtained by the simulations, Fig. 1(a), clearly mirrors the difference between Eqs. (13a) and (16a).

III. NONLINEAR COUPLINGS

For a more complete description of the LGA fluid macroscopic behavior we need to include in the constitutive relations the nonlinear contributions of the local equilibrium densities. In essence, we have to extend Eq. (10′) to include nonlinear effects.

The local conservation laws can be written as

$$\begin{aligned}\partial_t\langle n(\mathbf{r},t)\rangle&=-\partial_{x_m}\langle g_m(\mathbf{r},t)\rangle\ ,\\ \partial_t\langle g_i(\mathbf{r},t)\rangle&=-\partial_{x_m}\langle J_m^i(\mathbf{r},t)\rangle\ ,\\ \partial_t\langle h_a(\mathbf{r},t)\rangle&=-\partial_{x_m}\langle J_m^a(\mathbf{r},t)\rangle\ .\end{aligned} \tag{22}$$

In the equation above, $\langle\phi\rangle$ are the local equilibrium densities obtained by a suitable coarse-grained averaging procedure. Equation (22) is considered true in the long-wavelength limit; thus, in that expression, $\mathbf{r}$ and t are treated as continuous variables.

The dissipative contribution to the currents on the right-hand side of Eq. (22) has been discussed in Sec. II. The Eulerian, or nondissipative, part of the currents can be estimated as an expansion in the intensive parameters conjugated to g_m and h_a. For our purposes it is enough if the expression is truncated to the second order (see Appendix B). The resulting expression for $\langle J_m^a(\mathbf{r},t)\rangle$ is then (Appendix B)

$$\langle J_m^a(\mathbf{r},t)\rangle=\frac{\lambda}{2}(\delta_{mj}+2C_{a;m}^{\perp}C_{a;j}^{\perp})\langle g_j(\mathbf{r},t)\rangle\langle h_a(\mathbf{r},t)\rangle+(\kappa_1\delta_{mi}+\kappa_2C_{a;m}^{\perp}C_{a;i}^{\perp})\partial_{x_i}\langle h_a(\mathbf{r},t)\rangle\ . \tag{23}$$

The physical processes described in Eq. (23) are convection [by the $\langle g_i(v\mathbf{r},t)\rangle$] and diffusion, but neither of the corresponding terms in Eq. (23) has rotational symmetry. This should not be surprising since the staggered-momentum modes are very strongly tied, Eq. (2), to the microscopic structure of the model.

The current $\langle J_i^m(\mathbf{r},t)\rangle$ is given by

$$\langle J_i^m(\mathbf{r},t)\rangle=\delta_{mi}\langle p(\mathbf{r},t)\rangle+\lambda\left[\langle g_m(\mathbf{r},t)\rangle\langle g_i(\mathbf{r},t)\rangle+\sum_{a=1}^{3}C_{a;m}^{\perp}C_{a;i}^{\perp}\langle h_a(\mathbf{r},t)\rangle\langle h_a(\mathbf{r},t)\rangle\right]+\nu[\partial_{x_i}\langle g_m(\mathbf{r},t)\rangle+\partial_{x_m}\langle g_i(\mathbf{r},t)\rangle]+(\zeta-\nu)\delta_{mi}\partial_{x_k}\langle g_k(\mathbf{r},t)\rangle\ , \tag{24}$$

where the "pressure" p is given by

$$p(\mathbf{r},t)=c_s^2\langle n(\mathbf{r},t)\rangle-\lambda c_s^2(\tfrac{5}{6})[\langle g_m(\mathbf{r},t)\rangle\langle g_m(\mathbf{r},t)\rangle+\langle h_a(\mathbf{r},t)\rangle\langle h_a(\mathbf{r},t)\rangle]\ . \tag{25}$$

In the equation above, c_s^2 is the speed of sound for the gas, e.g., $c_s^2=\frac{3}{7}$ for the seven-velocity model FHP-III of Ref. 9, and $\lambda=(1-2d)/4\chi_s$.[1]

The constitutive equations presented in Eq. (24) show

some unexpected and striking features. In fact, Eq. (24) contains, together with a pressure term and a standard momentum convection term, a term that depends only on the $\langle h_a(\mathbf{r},t)\rangle$ densities. This term (together with a similar one concealed in the definition of p) makes the macroscopic behavior of the LGA fundamently differently from that of simple real fluids. In fact, the h modes can act as a source, through the presence term and/or the other term explicitly indicated in Eq. (24), for the $\langle g_m\rangle$ density. Hence the LGA can produce flow that are not the solution of the Navier-Stokes equation.

In the simulations reported thus far (with the exception of Refs. 23 and 24) there has been no clear indication of the presence of the staggered-momentum density h. This is not surprising since the initial conditions used had a negligible projection on the h modes, and the macroscopic flow does not [at the order of Eq. (23)] self-generate the h densities. Nonetheless, the non-Navier-Stokes effects described by Eq. (24) can be striking. In Fig. 2, I show the results of a simulation with "pathological" initial conditions $\langle h_2\rangle = h_0 \sin(2\pi y/W)$ and $g_m = 0$ in a two-dimensional box with periodic boundary conditions. The coordinate axes are oriented so that $\hat{\mathbf{x}} \| \mathbf{C}_1$ and the box is a parallelogram of width (y direction) W and length L. The curves plotted in Fig. 2 are the momentum density $\langle g_x\rangle$ versus y at successive times. The time derivatives $\partial_t \langle g_m\rangle$ measured in the simulations are in quantitative agreement with Eq. (24).[21] The actual size of the system used is $W=64$, $L=2$ and the simulation is performed using a recently developed Boltzmann-equation technique.[24]

IV. CONCLUSIONS

In the preceding sections, and especially in Eq. (24), we have seen that the macroscopic behavior of the LGA model currently used is richer than expected. There are six conserved quantities, three are the usual mass and momentum densities, the other three are the staggered-momentum densities h_a that are a peculiarity of the microscopic definition of the LGA.

The effects of the staggered momentum on the "flow" of the momentum and mass densities are not clear. It is easy to conceive "pathological" initial conditions (see Fig. 2) such that the macroscopic behavior of the LGA is qualitatively different from simple real fluid flows. On the other hand, it seems unlikely that the simulation setups commonly used[9,25,26] have, either in the initial conditions or while running, an appreciable projection on the h modes. The effects of a "controlled" injection of h on the initial conditions of a standard test flows, e.g., flow past a cylinder, are currently under study.[27]

The h-conserved densities are a peculiarity of the definitions of the LGA: particles occupying the sites of a regular lattice that can only hop between nearest neighbors. Thus the new hydrodynamic modes are very strongly tied to the microscopic structure of the model, cf. the anisotropy of κ, Eq. (15), and hence the "full" macroscopic behavior of the LGA does not seem to have any interesting physical application. The h_a can be easily destroyed. For instance, one could generalize the model to allow also for nearest-nearest neighbor hops. Unfortunately, I think that it would be very difficult to prove that this, or any other "simple" extension to the model, will remove any undesirable extensive conserved quantity. In fact, a closely related problem in lattice-gauge theory (doubling of the number of fermions modes) cannot easily be solved.[28]

The lattice-gas automaton has some very interesting qualities, e.g., intrinsic numerical stability; however, we are not guaranteed that the flow patterns produced by simulating it are automatically, apart from an essentially trivial rescaling, solutions of the Navier-Stokes equation. This does not imply that the lattice-gas automaton is not a feasible numerical technique, but rather that, as many other numerical methods, it requires some additional care in the analysis of the simulation results before it can be completely trusted.

ACKNOWLEDGMENTS

I am grateful to L. P. Kadanoff for his advice and insights, and to G. R. McNamara for many discussions. This work was partially supported by the U.S. Office of Naval Research, and it has been presented as a thesis to the Department of Physics, the University of Chicago, in partial fulfillment of the requirements for a Ph.D. degree.

APPENDIX A

Here I give some of the details of the calculation sketched in Sec. I. Since it is a rather straightforward application of Ref. 12, what appears below is just a brief summary of the formalism used and its application to the LGA.

1. Local equilibrium perturbations

In Sec. II, I defined the scalar product

$$\langle \Phi|\Psi\rangle = \sum_x \overline{\Phi}_x \Psi_x p_x^{\mathrm{eq}} , \tag{A1}$$

where p_x^{eq} is the equilibrium probability for the microscopic configuration x of the LGA system, Eq. (4). Equation (A1) suggests the formal vector notation

$$\begin{aligned} |f\rangle &= f|\mathrm{eq}\rangle = \sum_x p_x^{\mathrm{eq}} f_x |x\rangle , \\ \langle f| &= \sum_x \bar{f}_x \langle x| , \end{aligned} \tag{A2}$$

together with the convention $\langle x|y\rangle = \delta_{xy}$. The operator $\mathcal{L}$ applied to a "vector" means

$$\mathcal{L}|f\rangle = \mathcal{L}f|\mathrm{eq}\rangle = \sum_x p_x^{\mathrm{eq}} f_{\mathcal{L}^{-1}x} |x\rangle . \tag{A3}$$

The equilibrium "state" is invariant,

$$\mathcal{L}|\mathrm{eq}\rangle = |\mathrm{eq}\rangle , \tag{A4}$$

and

$$\langle f|\mathcal{L} = \sum_x \langle x|\bar{f}_{\mathcal{L}_x} . \tag{A5}$$

As in Ref. 12, I construct local equilibrium perturba-

tions to the equilibrium state Eq. (4) by adding, to the uniform value of the equilibrium intensive parameters, a small amplitude modulation with wave vector q, e.g.,

$$\alpha(\mathbf{r})=\alpha_0+(\epsilon/\sqrt{N})e^{-i\mathbf{q}\cdot\mathbf{r}} ,$$

$$|\text{loc eq}\rangle=Z[\alpha,\nu,\eta]^{-1}\exp\left[\sum_{\mathbf{r}'\in\Omega}\alpha(\mathbf{r})n(\mathbf{r})-\sum_{\mathbf{r}\in\Omega}\gamma(\mathbf{r})\cdot\mathbf{g}(\mathbf{r})-\sum_{\mathbf{r}\in\Omega}\eta_a(\mathbf{r})h_a(\mathbf{r})\right]\sum_x|x\rangle , \tag{A6}$$

and then keeping only up the first order in the expansion in ϵ of the perturbed state. The corrections to Eq. (4) due to the perturbation are then proportional to the vectors

$$|n(\mathbf{q})\rangle=\frac{1}{\sqrt{N}}\sum_{\mathbf{r}\in\Omega}e^{-i\mathbf{q}\cdot\mathbf{r}}(n(\mathbf{r})-n_0)|\text{eq}\rangle ,$$

$$|g_m(\mathbf{q})\rangle=\frac{1}{\sqrt{N}}\sum_{\mathbf{r}\in\Omega}e^{-i\mathbf{q}\cdot\mathbf{r}}g_m(\mathbf{r})|\text{eq}\rangle , \tag{A7}$$

$$|h_a(\mathbf{q})\rangle=\frac{1}{\sqrt{N}}\sum_{\mathbf{r}\in\Omega}e^{-i\mathbf{q}\cdot\mathbf{r}}h_a(\mathbf{r})|\text{eq}\rangle .$$

2. Microscopic currents

I will now systematically apply the evolution operator $\mathcal{L}$ to the local equilibrium perturbations of Appendix A 1. The purpose is to verify that Eqs. (A7) are a good approximation, up to $O(q)$, to eigenvectors of $\mathcal{L}$, and to compute the scalar products needed for formulas, Eqs. (11) and (12), of Sec. II. Using Eqs. (A3)–(A5) one obtains, neglecting terms of $O(q^3)$,

$$\mathcal{L}|n(\mathbf{q})\rangle=|n(\mathbf{q})\rangle+iq_m|g_m(\mathbf{q})\rangle-\frac{q_mq_k}{2}\mathcal{L}|J^m_k(\mathbf{q})\rangle ,$$

$$\mathcal{L}|g_m(\mathbf{q})\rangle=|g_m(\mathbf{q})\rangle+iq_k\mathcal{L}|J^m_k(\mathbf{q})\rangle+\frac{q_kq_j}{2}\mathcal{L}|J^m_{kj}(\mathbf{q})\rangle , \tag{A8}$$

$$\mathcal{L}|h_a(\mathbf{q})\rangle=-|h_a(\mathbf{q})\rangle+iq_m\mathcal{L}|J^a_m(\mathbf{q})\rangle+\frac{q_mq_k}{2}\mathcal{L}|J^a_{mk}(\mathbf{q})\rangle ,$$

together with their "adjoints"

$$\langle n(\mathbf{q})|\mathcal{L}=\langle n(\mathbf{q})|+iq_m\langle g_m(\mathbf{q})|-\frac{q_mq_k}{2}\langle J^m_k(\mathbf{q})| ,$$

$$\langle g_m(\mathbf{q})|\mathcal{L}=\langle g_m(\mathbf{q})|+iq_k\langle J^m_k(\mathbf{q})|-\frac{q_kq_j}{2}\langle J^m_{kj}(\mathbf{q})| , \tag{A9}$$

$$\langle h_a(\mathbf{q})|\mathcal{L}=-\left[\langle h_a(\mathbf{q})|+iq_m\langle J^a_m(\mathbf{q})|-\frac{q_mq_k}{2}\langle J^a_{mk}(\mathbf{q})|\right] ,$$

where the currents J^ϕ_m and their generalizations $J^\phi_{mk}\ldots$ are defined as

$$J^n_m(\mathbf{r})=g_m(\mathbf{r}) ,$$

$$J^n_{mk}(\mathbf{r})=J^m_k(\mathbf{r}) ,$$

$$J^m_{ki}\ldots(\mathbf{r})=\sum_a C_{a;m}C_{a;k}C_{a;i}\cdots(f_a(\mathbf{r})-d) ,$$

$$J^a_{ijk}\ldots(\mathbf{r})=(-1)^{\mathbf{B}_a\cdot\mathbf{r}}C^{\perp}_{a;m}J^m_{ijk}\ldots(\mathbf{r}) .$$

As advertized, the vectors defined in Eq. (A7) are, for $q\to0$, good approximations to eigenvectors of the Liouville operator $\mathcal{L}$ (cf. Sec. II B). The term proportional to q in Eq. (A8) represents the local conservation laws obeyed by the densities. However, the discrete nature of the lattice makes Eq. (A8) different from its continuous analog.[12] In fact, the currents that appear in Eq. (A8) are "retarded," i.e., $\mathcal{L}|J^\phi_m(\mathbf{q})\rangle$ rather than $|J^\phi_m(\mathbf{q})\rangle$, and there are also second-order corrections in the gradients which, as it is shown in Eq. (12), have an effect on the transport coefficients of the lattice-gas automata.

3. Equal-time correlation functions

The goal of the formalism presented in Sec. II is to express the linearized hydrodynamics of the system in terms of equal-time correlation functions, i.e., thermodynamic derivatives and transport coefficients. The probability distribution, Eq. (4), at the intensive parameters corresponding to $\langle\langle n\rangle\rangle=7d$ and $\langle\langle g_m\rangle\rangle=\langle\langle h_a\rangle\rangle=0$ completely factorizes on the sites and microscopic velocity directions and maintains the hexagonal symmetry of the lattice. Thus the equilibrium equal-time correlation functions can be easily evaluated. In fact, starting from

$$\langle\langle(f_a(\mathbf{r})-d)(f_{a'}(\mathbf{r}')-d)\rangle\rangle=d(1-d)\delta_{aa'}\delta_{\mathbf{r}\mathbf{r}'} , \tag{A10}$$

and using the hexagonal symmetry of the lattice, one quickly obtains, in the long-wavelength limit,

$$\langle\phi(\mathbf{q})|\phi'(\mathbf{q}')\rangle=\chi_\phi\delta_{\phi\phi'}\delta_{\mathbf{q}\mathbf{q}'} , \tag{A11}$$

where the label ϕ is n, g_m, or h_a and the susceptibilities χ_ϕ are $\chi_n=7d(1-d)$ and $\chi_g=\chi_h=3d(1-d)$. Using Eq. (A11) one can normalize the vectors, Eq. (A7), to $|\tilde{\phi}(\mathbf{q})\rangle=(1/\sqrt{\chi_\phi})|\phi(\mathbf{q})\rangle$.

4. Evaluation of the $L_{\phi\phi'}$ matrix

The matrix elements $\langle\phi(\mathbf{q})|\mathcal{L}\phi'(\mathbf{q})\rangle$ that appear in Eqs. (11) and (12) can now be readily evaluated. They have the structure

$$\langle\phi(\mathbf{q})|\mathcal{L}\phi'(\mathbf{q})\rangle=\delta_{\phi\phi'}+\frac{iq_m}{\sqrt{\chi_\phi\chi_{\phi'}}}\langle\phi(\mathbf{q})|J^{\phi'}_m(\mathbf{q})\rangle-\frac{q_mq_k}{2\sqrt{\chi_\phi\chi_{\phi'}}}\langle\phi(\mathbf{q})|J^{\phi'}_{mk}(\mathbf{q})\rangle . \tag{A12}$$

As I mentioned earlier the result is different from its continuous analog: the contribution $O(q^2)$ present in Eq. (A12) is a lattice effect only due to the streaming part of the LGA time evolution which, nonetheless, gives a correction to the LGA transport coefficients. To make

this transparent, $L_{\phi\phi'}$, Eq. (11), is defined as the $O(q)$ contribution of Eq. (A12), while the higher-order elements are absorbed in the definitions of $U_{\phi\phi'}$, Eq. (12).

5. Dissipative dynamics

The matrix elements

$$\tilde{U}_{\phi\phi'}=\langle\phi(\mathbf{q})|\mathcal{L}Q(\mathbf{q})\frac{1}{1-Q(\mathbf{q})\mathcal{L}Q(\mathbf{q})}Q(\mathbf{q})\mathcal{L}\phi'(\mathbf{q})\rangle \tag{A13}$$

require additional formal manipulation. One first notices that $\tilde{U}_{n\phi'}=\tilde{U}_{\phi n}=0$, then one can show, using

$$Q(\mathbf{q})\mathcal{L}|\Psi(\mathbf{q})\rangle=Q(\mathbf{q})\mathcal{L}Q(\mathbf{q})|\Psi(\mathbf{q})\rangle+O(q)\ , \tag{A14}$$

that

$$\tilde{U}_{lm}=-\frac{q_k q_j}{\chi_g}\left[\sum_{t=0}^{\infty}\langle J_k^l(\mathbf{q})|Q(\mathbf{q})\mathcal{L}^t Q(\mathbf{q})J_j^m(\mathbf{q})\rangle - \langle J_k^l(\mathbf{q})|J_j^m(\mathbf{q})\rangle\right], \tag{A15}$$

while

$$\tilde{U}_{ab}=-\frac{q_k q_j}{\chi_h}\left[\sum_{t=0}^{\infty}(-1)^t\langle J_k^a(\mathbf{q})|Q(\mathbf{q})\mathcal{L}^t Q(\mathbf{q})J_j^b(\mathbf{q})\rangle - \langle J_k^a(\mathbf{q})|J_j^b(\mathbf{q})\rangle\right]. \tag{A16}$$

Summing second-order correction terms of Eq. (A12) with Eq. (A13), one recovers Eq. (12) with

$$D_{ij}^{nn}=\frac{1}{2\chi_n}\langle n(\mathbf{q})|J_{ij}^n(\mathbf{q})\rangle=\frac{c_s^2}{2}\delta_{ij}\ ,$$

$$D_{ij}^{lm}=-\frac{1}{2\chi_g}\langle g_l(\mathbf{q})|J_{ij}^m(\mathbf{q})\rangle=-\tfrac{1}{8}(\delta_{lm}\delta_{ij}+2\delta_{li}\delta_{mj})\ , \tag{A17}$$

$$D_{ij}^{ab}=-\frac{1}{2\chi_h}\langle h_a(\mathbf{q})|J_{ij}^b(\mathbf{q})\rangle=-\frac{\delta_{ab}}{8}(\delta_{ij}+2C_{a;i}^{\perp}C_{a;j}^{\perp})\ ,$$

and $D^{nm}=D^{ni}=D^{ma}=0$. The speed of sound of the LGA, c_s, is defined by $c_s^2=\chi_g/\chi_n$.

6. Green-Kubo formulas

The expressions, Eq. (12), can be drastically simplified by using the underlying hexagonal symmetries of the lattice and assuming translational invariance. Thus one can rewrite

$$U_{lm}=q_k q_j[(\zeta-\nu)\delta_{lk}\delta_{mj}+\nu(\delta_{ml}\delta_{kj}+\delta_{mk}\delta_{lj})]\ ,$$

$$U_{ab}=q_k q_j\delta_{ab}C_{a;m}^{\perp}C_{a;l}^{\perp} \times[(\kappa_2-\kappa_1)\delta_{lk}\delta_{mj}+\kappa_1(\delta_{ml}\delta_{kj}+\delta_{mk}\delta_{lj})]\ , \tag{A18}$$

and show that $U_{al}=0$. The resulting Green-Kubo expressions for the transport coefficients κ_1, κ_2, ν and ζ are given in Sec. II, Eqs. (16)–(18). The lattice correction $\Gamma_s=\frac{1}{2}(\zeta_s+\nu_s)$ is not completely given by Eq. (A17). In fact, since the decay rate for the sound waves[29] is $s(q)=\pm icq+\Gamma q^2$, $\Gamma=\frac{1}{2}(\nu+\zeta)$, there is another lattice contribution of order q^2 concealed in the expansion of the term $e^{-s(q)}-1$ that effects the decay of sound waves and should then be incorporated in Γ_s.

APPENDIX B

In this Appendix I derive the local equilibrium, or Eulerian, contributions to the currents $\langle J_m^{\phi}(\mathbf{q})\rangle$. This is done as an expansion, up to second order, in the conserved densities, Eq. (6).

1. Intensive parameters

I start by rewriting the local equilibrium distribution, Eq. (A6), as

$$|\text{loc eq}\rangle=\frac{\exp\left[\alpha_0\sum_{\mathbf{r}\in\Omega}n(\mathbf{r})+\sum_{\mathbf{q}}\alpha(-\mathbf{q})\tilde{n}(\mathbf{q})-\boldsymbol{\gamma}(-\mathbf{q})\cdot\mathbf{g}(\mathbf{q})-\eta_a(-\mathbf{q})h_a(\mathbf{q})\right]}{Z[\alpha,\gamma_m,\eta_a]}\sum_x|x\rangle\ , \tag{B1}$$

where I split the intensive parameter $\alpha\to\alpha(\mathbf{q})+\alpha_0$, $\alpha(\mathbf{q}=0)=0$, α_0, such that $\langle\langle n(\mathbf{r})\rangle\rangle=n_0$, and define

$$\tilde{n}(\mathbf{q})=\frac{1}{\sqrt{N}}\sum_{\mathbf{r}\in\Omega}e^{-i\mathbf{q}\cdot\mathbf{r}}(n(\mathbf{r})-n_0)\ ; \tag{B2}$$

also

$$Z[\alpha,\gamma_m,\eta_\alpha]=\sum_x\langle x|\exp\left[\alpha_0\sum_{\mathbf{r}\in\Omega}n(\mathbf{r})+\sum_{\mathbf{q}}\alpha(-\mathbf{q})\tilde{n}(\mathbf{q})-\boldsymbol{\gamma}(-\mathbf{q})\cdot\mathbf{g}(\mathbf{q})-\eta_a(-\mathbf{q})h_a(\mathbf{q})\right]|x\rangle\ . \tag{B3}$$

Equations (23) and (24) of Sec. III are obtained in two steps. First I compute an expression, correct to the first order, for the intensive parameters in terms of the local equilibrium densities $\langle n\rangle$, $\langle g_m\rangle$, and $\langle h_a\rangle$. Then I use the value thus obtained for $\alpha,\boldsymbol{\gamma},\eta$ to evaluate $\langle J_m^{\phi}(\mathbf{q})\rangle$.

Before we consider the nonequilibrium average $\langle\ \rangle$, we need to express γ_m, η_a, and α in terms of the required local equilibrium fields $\langle\tilde{n}(\mathbf{q})\rangle$, $\langle g_m(\mathbf{q})\rangle$, and $\langle h_a(\mathbf{q})\rangle$,

$$\langle\tilde{n}(\mathbf{q})\rangle=\frac{Z[\alpha_0,0,0]}{Z[\alpha_0+\alpha,\boldsymbol{\gamma},\eta]}\left\langle\!\!\left\langle\tilde{n}(\mathbf{q})\exp\left[\sum_{\mathbf{q}'}\alpha(-\mathbf{q}')\tilde{n}(\mathbf{q}')-\boldsymbol{\gamma}(-\mathbf{q}')\cdot\mathbf{g}(\mathbf{q}')-\eta_a(-\mathbf{q}')h_a(\mathbf{q}')\right]\right\rangle\!\!\right\rangle$$

$$=\chi_n\alpha(\mathbf{q})+\frac{(1-2d)\chi_g}{2}\sum_{\mathbf{q}'}\boldsymbol{\gamma}(\mathbf{q}-\mathbf{q}')\cdot\mathbf{g}(\mathbf{q}')+\eta_a(\mathbf{q}-\mathbf{q}')\eta_a(\mathbf{q}')\ , \tag{B4}$$

where I used

$$\frac{Z[\alpha_0+\alpha,\gamma,\eta]}{Z[\alpha_0,0,0]}=\left\langle\!\left\langle \exp\left[\sum_{\mathbf{q}}\alpha(-\mathbf{q})\tilde{n}(\mathbf{q})-\gamma(-\mathbf{q})\cdot\gamma(\mathbf{q})-\eta_a(-\mathbf{q})h_a(\mathbf{q})\right]\right\rangle\!\right\rangle$$
$$=1+O(\gamma^2,\eta^2)\ , \tag{B5}$$

and neglected higher orders of γ,η in Eq. (B4). At the same order,

$$\langle g_m(\mathbf{q})\rangle=-\chi_g\gamma_m(\mathbf{q}),\quad \langle h_a(\mathbf{q})\rangle=-\chi_h\eta_a(\mathbf{q})\ . \tag{B6}$$

Equations (B4) and (B6) can then be solved for $\alpha(\mathbf{q})$, $\gamma(\mathbf{q})$, and $\eta_a(\mathbf{q})$.

2. Euler constitutive relations

The current

$$\langle J_i^m(\mathbf{q})\rangle=\left\langle\!\left\langle J_i^m(\mathbf{q})\exp\left[\sum_{\mathbf{q}'}\alpha(-\mathbf{q}')\tilde{n}(\mathbf{q}')-\gamma(-\mathbf{q}')\cdot\gamma(\mathbf{q}')-\eta_a(-\mathbf{q}')h_a(\mathbf{q}')\right]\right\rangle\!\right\rangle \tag{B7}$$

can then be expanded up to second order in γ,η,α to obtain

$$\langle J_i^m(\mathbf{q})\rangle=\tfrac{1}{2}\sum_{\mathbf{q}',\mathbf{q}''}\alpha(\mathbf{q}')\alpha(\mathbf{q}'')\left\langle\!\left\langle\frac{\partial^2 J_i^m(\mathbf{q})}{\partial\alpha(\mathbf{q}')\partial\alpha(\mathbf{q}'')}\right\rangle\!\right\rangle+\gamma_i(\mathbf{q}')\gamma_j(\mathbf{q}'')\left\langle\!\left\langle\frac{\partial^2 J_i^m(\mathbf{q})}{\partial\gamma_i(\mathbf{q}')\partial\gamma_j(\mathbf{q}'')}\right\rangle\!\right\rangle+\eta_a(\mathbf{q}')\eta_b(\mathbf{q}'')\left\langle\!\left\langle\frac{\partial^2 J_i^m(\mathbf{q})}{\partial\eta_a(\mathbf{q}')\partial\eta_b(\mathbf{q}'')}\right\rangle\!\right\rangle\ . \tag{B8}$$

The thermodynamic derivatives above can be easily evaluated (see Appendix A 3) and Eq. (B8) can be simplified to

$$\langle J_i^m(\mathbf{q})\rangle=\delta_{mi}p(\mathbf{q})+\frac{\lambda}{\sqrt{N}}\sum_{\mathbf{q}'}[\langle g_m(\mathbf{q}-\mathbf{q}')\rangle\langle g_i(\mathbf{q}')\rangle+C^{\perp}_{a;m}C^{\perp}_{a;i}\langle h_a(\mathbf{q}-\mathbf{q}')\rangle\langle h_a(\mathbf{q}')\rangle]\ , \tag{B9}$$

where the pressure

$$p(\mathbf{q})=c_s^2\langle\tilde{n}(\mathbf{q})\rangle-\frac{\lambda c_s^2}{\sqrt{N}}\left[\frac{5}{6}\right]\sum_{\mathbf{q}'}[\langle g_m(\mathbf{q}-\mathbf{q}')\rangle\langle g_m(\mathbf{q}')\rangle+\langle h_a(\mathbf{q}-\mathbf{q}')\rangle\langle h_a(\mathbf{q}')\rangle+\frac{12c_s^2}{5}\langle\tilde{n}(\mathbf{q}-\mathbf{q}')\rangle\langle\tilde{n}(\mathbf{q}')\rangle]\ , \tag{B10}$$

and I neglect higher-order contributions. $c_s^2=\chi_g/\chi_n$ is the speed of sound for the LGA, e.g., in the seven-velocity model[9] $c_s^2=\frac{3}{7}$, while $\lambda=(1-2d)/12d(1-d)$. The term proportional to $\langle\tilde{n}\rangle^2$ present in Eq. (B10) is kept for formal consistency. In the actual simulations, $\langle\tilde{n}\rangle$ balances the $\langle g_m\rangle^2$ and $\langle h_a\rangle^2$ terms of the pressure equation, Eq. (B10). Hence $\langle\tilde{n}\rangle^2$ became a fourth-order term in $\langle g_m\rangle$ and $\langle h_a\rangle$ that can be neglected.

With similar manipulations one obtains

$$\langle J_m^a(\mathbf{q})\rangle=\frac{\lambda}{2\sqrt{N}}\sum_{\mathbf{q}'}(\delta_{mi}+2C^{\perp}_{a;m}C^{\perp}_{a;i})\times\langle g_i(\mathbf{q}-\mathbf{q}')\rangle\langle h_a(\mathbf{q}')\rangle\ . \tag{B11}$$

Equations (B9)–(B11) can then be Fourier transformed back to Eqs. (23)–(25).

*Present address: Program in Applied & Computational Mathematics, Princeton University, Princeton, NJ 08544.

[1]U. Frisch, B. Hasslacher, and Y. Pomeau, Phys. Rev. Lett. **56**, 1505 (1986).
[2]U. Frisch, D. d'Humières, B. Hasslacher, P. Lallemand, Y. Pomeau, and J.-P. Rivet, Complex Syst. **1**, 648 (1987).
[3]S. D. Kugelmass, R. Squier, and K. Steiglitz, Complex Syst. **1**, 939 (1987).
[4]J. L. Lebowitz, E. Presutti, and H. Spohn, J. Stat. Phys. **51**, 841 (1988).
[5]S. S. Orszag and V. Yakhot, Phys. Rev. Lett. **56**, 1691 (1986).
[6]S. Zaleski (unpublished).
[7]S. Wolfram, J. Stat. Phys. **45**, 471 (1986).
[8]G. McNamara and G. Zanetti (unpublished).
[9]D. d'Humières and P. Lallemand, C. R. Acad. Sci. Paris **302**, 983 (1986).
[10]The new conserved quantities have a formal resemblance to the staggered magnetization in isotropic antiferromagnets. However, the physics behind the two problems is deeply different. In fact, h_a is a true conserved density and it does not correspond to any continuously broken symmetry. R. Freeman and G. F. Mazenko, Phys. Rev. B **13**, 4967 (1976); see also, Ref. 11.
[11]B. I. Halperin, P. C. Hohenberg, and E. D. Siggia, Phys. Rev. B **13**, 1299 (1976).
[12]L. P. Kadanoff and J. Swift, Phys. Rev. **166**, 89 (1968).
[13]L. P. Kadanoff and P. Martin, Astrophys. J. **24**, 419 (1963).
[14]L. Kadanoff, Phys. Today **39** (9) (1986).
[15]J.-P. Rivet and U. Frisch, C. R. Acad. Sci. Paris **302**, 267 (1986).
[16]Strictly speaking H is actually conserved only for particularly simple boundary conditions; on the other hand, in the limit of large Ω these boundary effects become irrelevant.
[17]U. Frisch and J.-P. Rivet, C. R. Acad. Sci. Paris **303**, 1065 (1986).
[18]M. Henon, Complex Syst. **1**, 762 (1987).

[19]L. P. Kadanoff, G. McNamara, and G. Zanetti (unpublished).
[20]L. P. Kadanoff, G. R. McNamara, and G. Zanetti, Complex Syst. **1**, 791 (1987).
[21]G. Zanetti (unpublished).
[22]J.-P. Rivet, Ph.D. thesis, Ecole Normale Supérieure, Université de Paris VII, 1988.
[23]M. E. Colvin, A. J. C. Ladd, and B. J. Alder, Phys. Rev. Lett. (to be published).
[24]G. McNamara and G. Zanetti, Phys. Rev. Lett. **61**, 2332 (1988).
[25]D. d'Humières and P. Lallemand, Physica A **140**, 326 (1986).
[26]J.-P. Rivet, M. Henon, U. Frisch, and D. d'Humières, Europhys. Lett. **7**, 231 (1988).
[27]G. McNamara and G. Zanetti (unpublished).
[28]*Recent Advances in Field Theory and Statistical Mechanics,* Proceedings of the Les Houches Summer School, Session XXXIX, edited by J. B. Kogut, B. Zuber, and R. Stora (Elsevier Science, New York, 1984), pp. 319–460.
[29]L. Landau and E. Lifshitz, *Fluid Mechanics* (Pergamon, New York, 1986).